ARRIVAL STRUCTURE OF LONG-RANGE PROPAGATION EXCITED BY A FINITE AMPLITUDE SOURCE

W. A. Kuperman[1], B. E. McDonald[2] and G. L. D Spain[1]

[1]University of California, San Diego, [2]Naval Research Laboratory

ABSTRACT

We have studied the group and phase speed structure of long-range acoustic arrivals using linear acoustics. Here we present a preliminary study of some of these same paths but now we consider a higher amplitude source necessitating a nonlinear acoustic treatment. This research involves the eventual coupling of the Nonlinear Progressive Wave Equation (NPE) with an Adiabatic Normal Mode (ANM) Model. We use the ANM model (which has limited range-dependent capability) because our previous treatment for the linear problem was very revealing with respect to the physics of the arrival structure.

KEY WORDS: acoustic arrival, nonlinear progressive wave equation, hydroacoustic

OBJECTIVE

The objective of this work is to derive new technologies, based on the physics of underwater sound propagation (both linear and nonlinear), for localizing underwater sound sources using data from single hydrophone stations that are part of the International Monitoring System.

RESEARCH ACCOMPLISHED

Introduction

According to linear acoustic theory, the arrival structure of a pulse propagating a long distance in the ocean is a result of the relationship between group speed and phase speed of its various components, the latter often characterized as the frequency dependent normal modes, or more simply, acoustic multipaths (Kuperman et al, 2001). In particular, it is the appropriately integrated group speed over the individual acoustic/geographic paths that are important, and the arrival structure therefore contains source property information including its location. This group-vs-phase speed property is, in linear acoustics, independent of source amplitude. Even though the nonlinear or amplitude-dependent regime becomes more complicated, the original nonlinear nature of the source may remain as a scar in the received long distance linear arrival. The goal of this research is to address the possibility of this potential diagnostic. This paper outlines some of the basic linear-vs-nonlinear issues and presents some initial calculations illustrating these points.

Group Speed vs Phase Speed in Linear Acoustics

Though global acoustic propagation can occur only in deep water, we must include coastal or shallow water, bottom reflecting environments because of the potential location of a high amplitude source. The classic group/phase speed representation in shallow water is the so-called Pekeris curves (Jensen et al, 1994) shown in Figure 1 for modal propagation:

We are basically interested in the regime to the right of the minimum (Airy phase) of the group speed curves. Here we see that when phase speed increases, group speed decreases corresponding to a positive waveguide invariant β (Chuprov, 1982; Brekhovskiskh and Lysanov, 1991; D'Spain and Kuperman, 1999). Physically, this can be easily explained in terms of paths with higher angles with respect to the horizontal, and therefore, large

(horizontal) phase speeds, propagate energy at lower speeds.

On the other hand, the set of deep water paths shown in Figure 2 have more diversity in their group-vs-phase speed dependence. Bottom bounce paths have the same relation as above, but the deep refracting paths, such as the RR and RSR paths typically have the opposite group-vs-phase speed dependence. That is, group speed increases with increasing phase speed ($\beta < 0$) because the deep paths refract in water column regions of higher speed as opposed to the bottom reflection case in which a reflection occurs before a path can reach a sufficiently higher speed region in which the net effect over the path is to increase the group speed. In realistic ocean environments, the sound speed varies with range such as the climatology data associated with recent ATOC experiments (Worcester et al, 1991; ATOC Consortium, 1998; Worcester et al, 1999; Colosi, et al, 1999; Heaney and Kuperman, 1998) shown in Figure 3. We must then calculate the effective group speed over the whole path. An adiabatic normal mode computation (Jensen et al, Heaney et al, 1991) is often adequate, where, in addition, we approximate the phase speed to be a continuous variable because of the typically large number of modes, whereas in reality there is a discrete distribution of modes.

The local phase speed of the nth mode at the source location (which corresponds to a launch angle) is related to the modal wavenumber k_n,

$$c_{pn}(\omega) = \frac{\omega}{k_n},\qquad(1)$$

where ω is the angular frequency of the propagating acoustic mode. In a range-dependent environment, we must derive an effective average modal group speed, u_n, from the range-averaged slowness. That is, we note that the pulse observables at range r are arrival times that are given by r/u_n. Hence, for a range-dependent environment we are concerned with $1/u_n \equiv \bar{s}_{gn}$ where the overbar denotes range averaging and s_{gn} is referred to as the (local) modal group slowness. Since the adiabatic mode approximation has a range-averaged modal wavenumber associated with each term, it follows that (Jensen et al, 1994)

$$\overline{s_{gn}(r,\omega)} = \frac{\partial}{\partial\omega}\left(\frac{1}{r}\int_0^r k_n(r',\omega)dr'\right)\qquad(2)$$

and the range-dependent effective group speed is,

$$<u_n(r,\omega)> = \overline{\overline{\frac{1}{s_{gn}(r,\omega)}}}\qquad(3)$$

Hence, the range-dependent effective group speed is obtained from the harmonic average:

$$\frac{1}{\langle u_n(r,\omega)\rangle} = \frac{1}{r}\sum_{\Delta r'_n}\frac{\Delta r'_n}{u_n(r',\omega)}\qquad(4)$$

where the sum is taken over the approximate n range-independent subintervals, $\Delta r'_n$, of the propagation path. Finally, we note that we can interchange the partial with the integral sign in Eq. 2 and can use the modal formula for the (local or range-independent) modal group speed (Jensen et al, 1994),

$$\frac{\partial k_n}{\partial\omega} = \frac{1}{u_n(\omega)} = \frac{\omega}{k_n(\omega)}\int_0^\infty \frac{p^2_n(\omega;z)}{\rho(z)c^2(z)}dz,\qquad(5)$$

where $p_n(\omega;z)$ are the normal mode eigenfunctions of the pressure field in the ocean waveguide and $\rho(z)$ and $c(z)$ are the density and sound speed profiles as a function of depth.

Applying Eq. (4) to the data in Figure 3, we obtain the effective group speed (at a final specified range) vs phase speed (g-v) curves parameterized by frequency shown in Figure 4. These curves are actually a summary of the expected pulse arrival structure. Thus, for example, we should see three dominant features in the arrival structure. At the lowest phase speed, we note that all the modal group speeds are independent of frequency and these components have the same and lowest group speed. Hence, there should be a high-intensity last arrival since all components arrive at the same time. Next there should another high-intensity arrival (RR/RSR) region

corresponding to a phase and group speed of (1516 km/s, 1483.6 km/s). At this coordinate there is a stationary region for a group of modes (Kuperman et al, 2001). Finally, there is the region on the upper right that cuts off (to dispersive, lossy bottom interacting modes. This high group speed region, which describes the fastest paths (earliest arrivals) should be low in amplitude. The above is descriptive of the experimental results for this ATOC path shown in Figure 5.

Finally, with respect to linear acoustics, we mention that, as described above, since shallow and deep water propagation have different g-v curves, a transition from shallow to deep water will have a profound effect on the arrival structure. This can be seen from Eq. (4), which states that the effective group speed is an average over group slowness. That is, group speeds add like parallel resistors and so a small continental shelf region will have a large effect on the arrival structure. Hence, we have a linear diagnostic for sources originating in shallow vs deep water regions.

Nonlinear Propagation Effects

Large amplitude sources produce nonlinear effects in which super-position principle breaks down and new frequencies are generated. These effects, even after decay to the linear acoustic regime, remain as possible diagnostics of high-energy sources. In this section, we summarize some of the nonlinear waveguide effects that we expect will be useful. We will base the discussion on the Nonlinear Progressive Wave Equation (NPE) (McDonald and Kuperman, 1985; McDonald and Kuperman, 1987).

The NPE is based on a first-order nonlinear wave equation bearing the same relation to hydrodynamic compressional waves that the Korteweg - de Vries (KdV) equation bears to weakly nonlinear incompressible waves in water. The NPE is cast in a pulse-tracking frame of reference translating at a speed approximating the speed of sound (see Figure 6), and includes lowest order compressional nonlinearity along with diffraction and refraction. For appropriate environments, it possesses similarity solutions (McDonald and Ambrosiano, 1988) analogous to the solitary wave solutions of the KdV equation.

Normally we use pressure in linear acoustics, but it has been convenient to derive the NPE in terms of density; let $R_1(\mathbf{r}, t)$ be a linear baseline acoustic solution, then the NPE for quadratic nonlinearity is given by

$$(c_0^{-1}\partial_t + \partial_r + \frac{1}{2r})R_2 = -\alpha R_1 \, \partial_r R_1; \tag{6}$$

where, α is the coeffcient of nonlinearity. With the modal sum expressed in the time domain

$$R_1(r,z,t) = \sum_n A_n(r)\psi_n(z)\cos(k_n r - \omega t + \phi_n), \tag{7}$$

we obtain, after substantial mathematical manipulation, a nonlinear modal propagation equation for the depth integrated field,

$$\int dz R_2 = \alpha \sum_n \frac{a_n(r)^2 k_n}{2} Q(\theta_n)\sin 2(k_n r' + \varphi_n) \tag{8}$$

where the actual form of Q is given elsewhere (McDonald, 2002). The important point here is the generation of harmonics. This result is a particular simple form obtained by restricting the background environment to an analytical, convergence zone generating sound speed profile. Here we begin to see solutions that exhibit the modal behavior that must accompany nonlinear acoustic propagation; that is, the emergence of harmonics. This idealized result, shown in Figure 7, indicates that the vertically integrated second harmonic maximizes near odd number convergence zones and represents an example of the expected departure from linear results of the previous section.

The nonlinear tendency toward greater bottom interaction has been documented elsewhere (Ambrosiano et al, 1990) using the NPE. This would alter the modal excitation spectrum toward bottom interacting acoustic modes. That is, wavefront steepening shifts the source spectrum toward higher frequency, while Mach reflection increases bottom interaction. A schematic modal frequency - arrival time diagram, shown in Figure 8, illustrates that bottom interaction gives rise to clustered low-frequency arrivals before the final deep water axial cutoff (the lowest group speed). Figure. 9 shows a plot for another ATOC example to be considered in the context of Figure 8. Thus, one evidence of a nonlinear event in the water column could be the appearance of

another focal spot at low frequency in Figure 9 corresponding to the arrival of the bottom interacting modes vs the already existing surface interacting focal region at 2010 seconds. This suggests that we may be able to fold nonlinear effects into a g-v, albeit amplitude dependent, type summary of the propagation conditions.

CONCLUSIONS AND RECOMMENDATIONS

We have shown that the group speed dependence on phase speed (g-v curves) is diagnostic of the arrival structure of a long -distance propagating pulse governed by linear acoustics. Further, we have shown that the effective group speed results from averaging slowness. The different g-v structure in shallow and deep water will show up in the received arrival structure of a pulse traveling between shallow and deep water. Finally, we have also demonstrated that nonlinear modal propagation redistributes the modal acoustic energy and hence the integrated group speeds. Our next goal is to cast these nonlinear results in the analogous g-v structure we have set up for the linear case.

REFERENCES

Ambrosiano, J., D. R. Plante, B. E. McDonald, and W. A. Kuperman (1990), Nonlinear Propagation in an Ocean Waveguide , *J. Acoust. Soc. Am*. 87, 1473 - 1481.

ATOC Consortium (1998), Ocean Climate Change: Comparison of Acoustic Tomography, Satellite Altimetry, and Modeling , *Science* 281,1327-1332.

Brekhovskikh, L. M. and Y. P. Lysanov (1991), *Fundamentals of Ocean Acoustics*, 2nd ed., Springer-Verlag, New York (1991).

Chuprov, S. D. (1982), Interference structure of a sound field in a layered ocean, in *Ocean Acoustics, Current State*, ed. by L. M. Brekhovskikh, I. B. Andreevoi: Nauka, Moscow, 71-91.

Colosi, J. A., E. K. Sheer, S. Flatte, B. D. Cornuelle, M. A. Dzieciuch, W.H. Munk, P. F. Worcester, B. M. Howe, J.A. Mercer, R.C. Spindel, K. Metzger, T. G. Birdsall and A.B. Baggeroer (1999), Comparisons of measured and predicted acoustic fluctuations for a 3250-km propagation experiment in the eastern North Pacific," *J. Acoust. Soc. Am*., 105(6), 3202-3218.

D'Spain, G. L. and W. A. Kuperman (1999), Application of waveguide invariants to analysis of spectrograms from shallow water environments that vary in range and azimuth , *J. Acoust. Soc. Am*., 106(5), 2454-2468.

Heaney, K. D. and W. A. Kuperman (1998), Very long-range source localization with a small vertical array , *J. Acoust. Soc. Am*. 104(4), 2149-2159.

Heaney, K. D., W. A. Kuperman and B. E. McDonald (1991), Perth- Bermuda sound propagation (1960): Adiabatic Mode Interpretation, *J. Acoust. Soc. Am*. 90, 2586-2594.

Jensen, F. B., W. A. Kuperman, M. B. Porter and H. Schmidt (1994), Computational Ocean Acoustics, AIP Press, Woodbury, N.Y.

Kuperman, W. A., G. L. D Spain and K. D. Heaney, (2001), Long range source localization from single hydrophone spectrograms, *J. Acoust. Soc. Am*. 109, 1935-1943.

McDonald, B. E. and W. A. Kuperman (1985), Time Domain Solution of the Parabolic Equation Including Nonlinearity *J. Comp. Math. w. Appl.* 11, 843 - 851.

McDonald, B. E. and W. A. Kuperman (1987), Time Domain Formulation for Pulse Propagation Including Nonlinear Behavior at a Caustic, *J. Acoust. Soc. Am*. 81, 1406 - 1417.

McDonald, B. E. and J. Ambrosiano (1988) Similarity Solution for Low Mach Number Spherical Shocks , *J. Acoust. Soc. Am*. 84, 1497 -1503.

McDonald, B. E. (2002), Nonlinear Effects in Source Localization , in *Ocean Acoustic Interference Phenomena*, eds. W. A. Kuperman and G. L. D Spain, AIP Press, NY.

Worcester, P. F., B. D. Cornuelle, J. A. Hildebrand, W. S. Hodgkiss, T, F. Duda, J. Boyd, B. M. Howe, J. A. Mercer, and R. C. Spindel (1991), A comparison of measured and predicted broadband acoustic arrival patterns in travel time-depth coordinates at 1000 km range , *J. Acoust. Soc. Am*., 95(6), 3118-3129.

Worcester, P. F., B.D. Cornuelle, M.A. Dzieciuch, W.H. Munk, B. M. Howe, J.A. Mercer, R.C. Spindel, J.A. Colosi, K. Metzger T. G. Birdsall and A.B. Baggeroer (1999), A test of basin-scale 13 acoustic thermometry using a large-scale vertical array at 3250-km range in the eastern North Pacific , *J. Acoust. Soc. Am*., 105(6), 3185-3201.
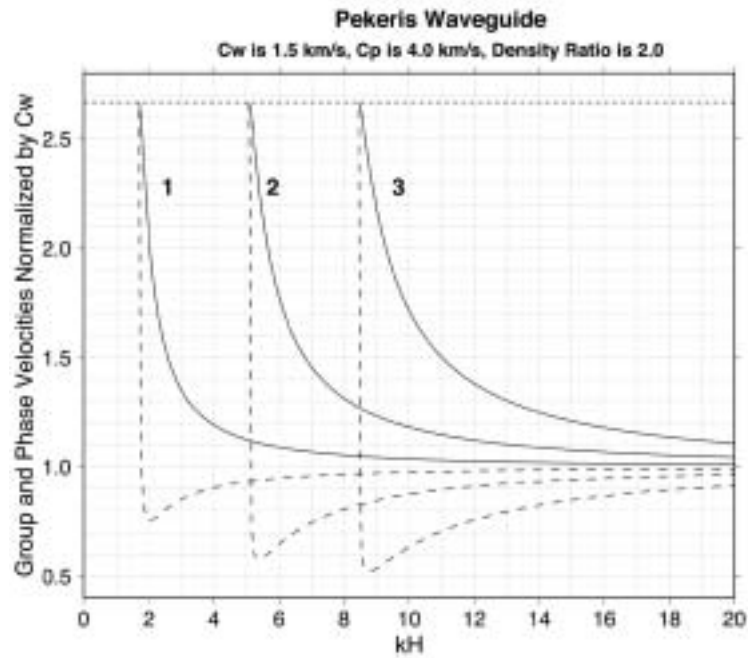
Figure 1: Dispersion curves for Pekeris waveguide.
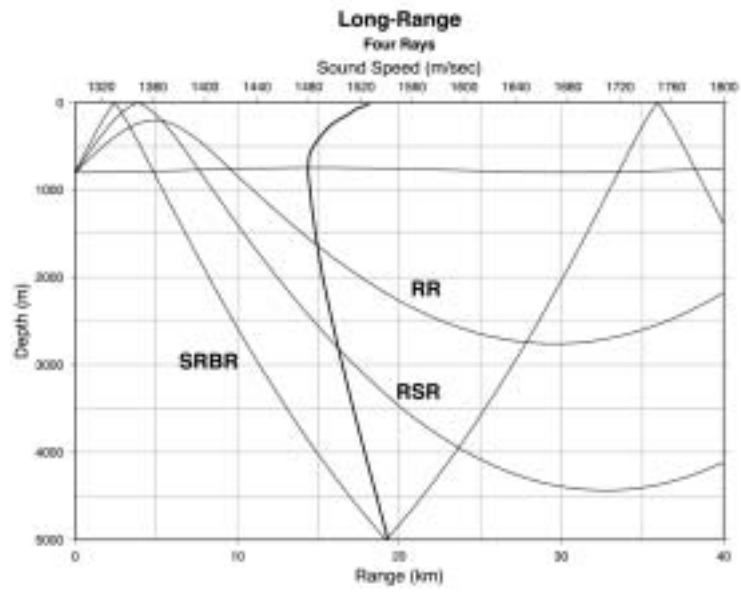
Figure 2: Schematic of deep water paths.
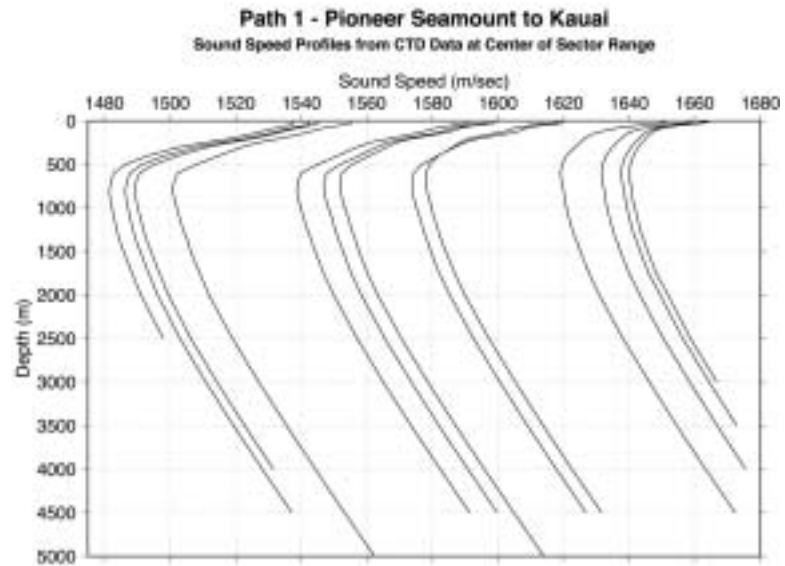
Figure 3: Sound speed profiles for a 3500 km ATOC propagation path as obtained from a climatology data base.
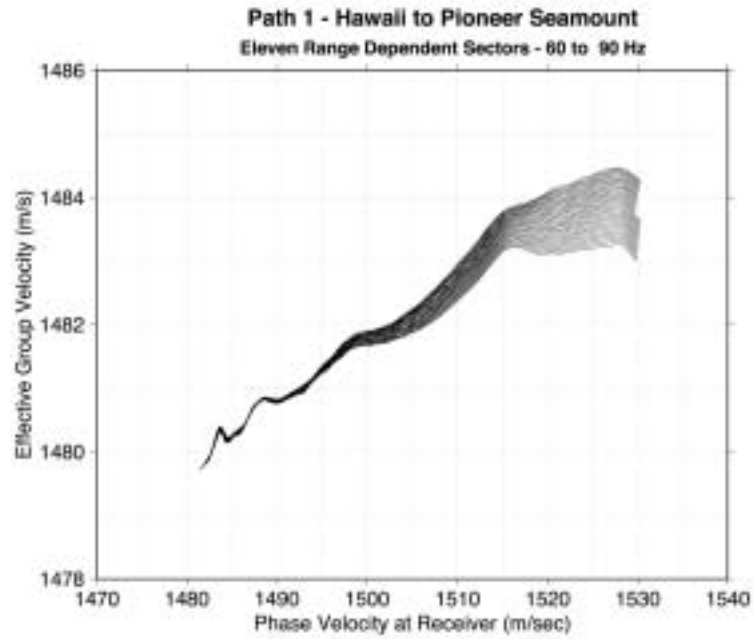
Figure 4: Group speed vs phase speed (g-v) curves for the climatology derived sound speeds of Figure 3.
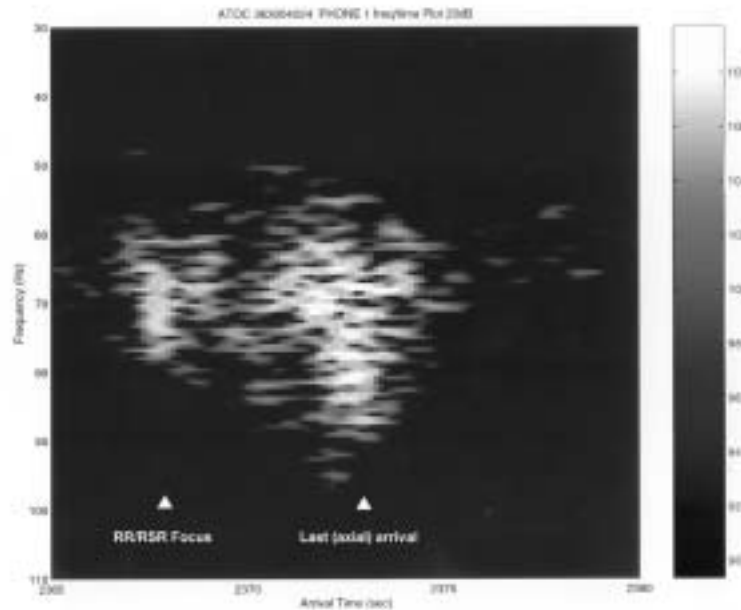

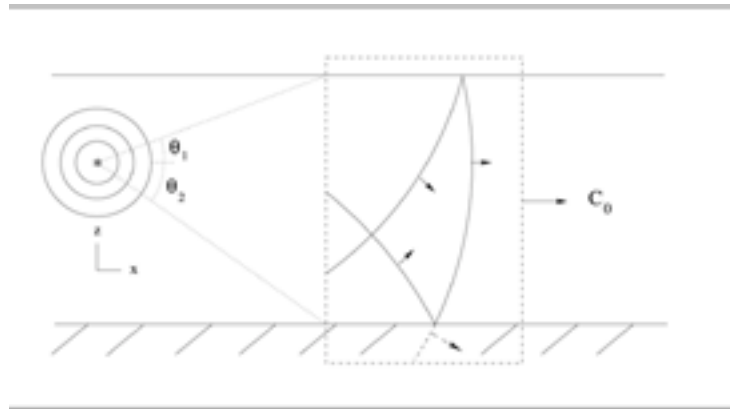Figure 5:   ATOC data: The pulse arrival structure corresponding to Figs. 4 and 5.

Figure 6:   The geometry for the Nonlinear Progressive Wave Equation (NPE)
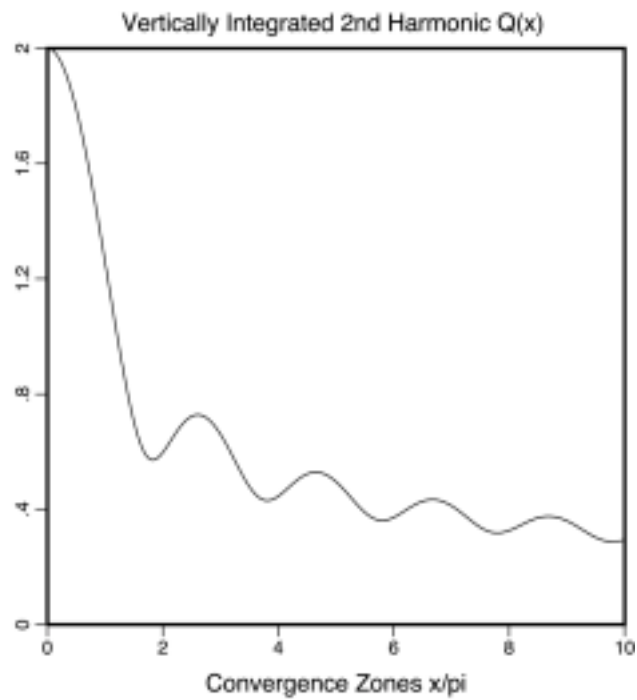
Figure 7:   Second harmonic of a high amplitude source for the particular case of a parabolic slowness profile
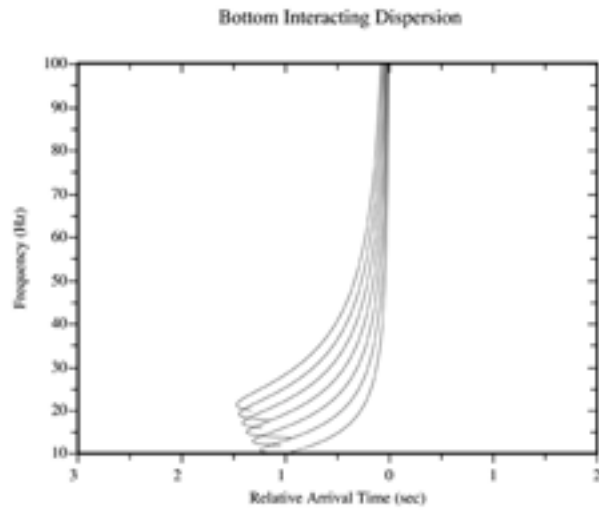has local maxima near odd number convergence zones

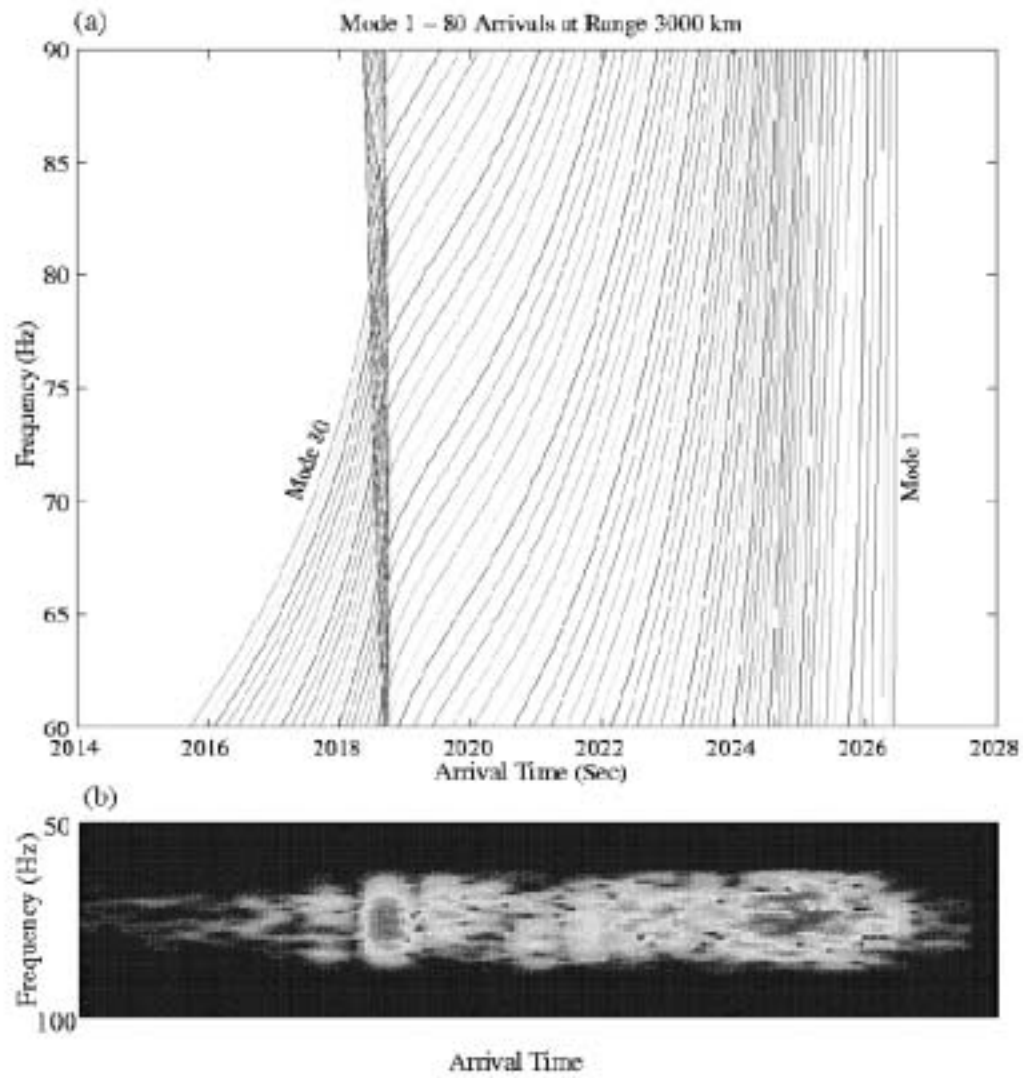Figure 8:   Dispersion curves for a set of bottom interacting modes

Figure 9: Modal dispersion and arrival structure for an ATOC propagation example.